Preprint
UCRL-JC-147739

Downstream System for the Second Axis of the Darht Facility

Y.-J. Chen, et. al

This article was submitted to
XXI International LINAC Conference, Gyeongju, South Korea,
August 19-23, 2002

July 15, 2002

U.S. Department of Energy

Lawrence
Livermore
National
Laboratory

DOWNSTREAM SYSTEM FOR THE SECOND AXIS OF THE DARHT FACILITY*

Yu-Jiuan Chen, L. R. Bertolini, G. J. Caporaso, F. W. Chambers, E. G. Cook, S. Falabella, F. J. Goldin, G. Guethlein, D. D.-M. Ho, J. F. McCarrick, S. D. Nelson, R. Neurath, A. C. Paul, P. A. Pincosy, B. R. Poole, R. A. Richardson, S. Sampayan, L.-F. Wang, J. A. Watson, G. A. Westenskow, and J. T. Weir
LLNL, Livermore, CA 94550, USA

Abstract

This paper presents the physics design of the DARHT-II downstream system, which consists of a diagnostic beam stop, a fast, high-precision kicker system and the x-ray converter target assembly. The beamline configuration, the transverse resistive wall instability and the ion hose instability modelling are presented. We also discuss elimination of spot size dilution during kicker switching and implementation of the foil-barrier scheme to minimize the backstreaming ion focusing effects. Finally, we present the target converter's configuration, and the simulated DARHT-II x-ray spot sizes and doses. Some experimental results, which support the physics design, will be also presented.

1 INTRODUCTION

The second-axis of the Dual Axis Radiographic Hydrodynamic Test facility (DARHT-II) will perform multiple-pulse (1 - 4 pulses) x-ray flash radiography [1]. The DARHT-II accelerator will deliver an 18.4-MeV (± 0.5 % over the flattop), 2-kA (± 1 %), 2-μs, 1000 mm-mr (Lapostolle emittance) beam. These beam parameters make the DARHT-II downstream system the first system ever designed to transport a high current, high energy and long pulse beam [2], [3]. Designing the DARHT-II downstream system is challenging. Instabilities caused by resistivity of the wall material and focusing effects due to beam-induced ionization of the background gas could potentially threaten the beam quality in the long drift sections of the system. A static x-ray converter target will be used on DARHT-II to preserve the radiographic axis. Having enough target material for all four beam pulses to generate the required X-ray doses provides a new challenge. To achieve the radiographic performance specifications, the time integrated beam spot size on the target for all pulses (10 – 100 ns long) should be within 2.1 mm (50% MTF definition). However, the interactions between the high energy intensity beam with the target may disrupt the beam spot size.

The DARHT-II beamline configuration is presented in Sec. 2. The transverse resistive wall instability and the ion hose instability modelling are presented in Sec. 3. Discussion of elimination of spot size dilution during kicker switching is given in Sec. 4. Implementation of the foil-barrier scheme to minimize the backstreaming ion focusing effects is discussed in Sec. 5. The target converter's configuration, and the simulated DARHT-II x-ray spot sizes and doses are presented in Sec. 6. Finally, a summary is given in Sec. 7.

• This work was performed under the auspices of the U.S. Department of Energy by University of California Lawrence Livermore National Laboratory under contract No. W-7405-Eng-48.

2 BEAMLINE CONFIGURATION

The DARHT-II downstream system, shown in Fig.1, consists of a diagnostic beam stop, a high-speed, high-precision kicker system [4] and the x-ray converter target assembly [3], [4]. The kicker is used to select multiple short current pulses out of the long beam pulse provided by the accelerator. The nominal beam pulse length in the transport line upstream of the quadrupole septum (~ 12 m) and in the main beam dump line is 2 μs. Only the selected short beam pulses will be delivered to an x-ray converter target (~10 m) to produce high quality x-ray pulses. The nominal beam envelope in the target line is shown in Fig. 2. The remaining unkicked electron beam will be delivered to a beam dump. When the diagnostic beam stop is inline, the beamline configuration provides the capability for diagnosing emittance of the beam exiting the accelerator.

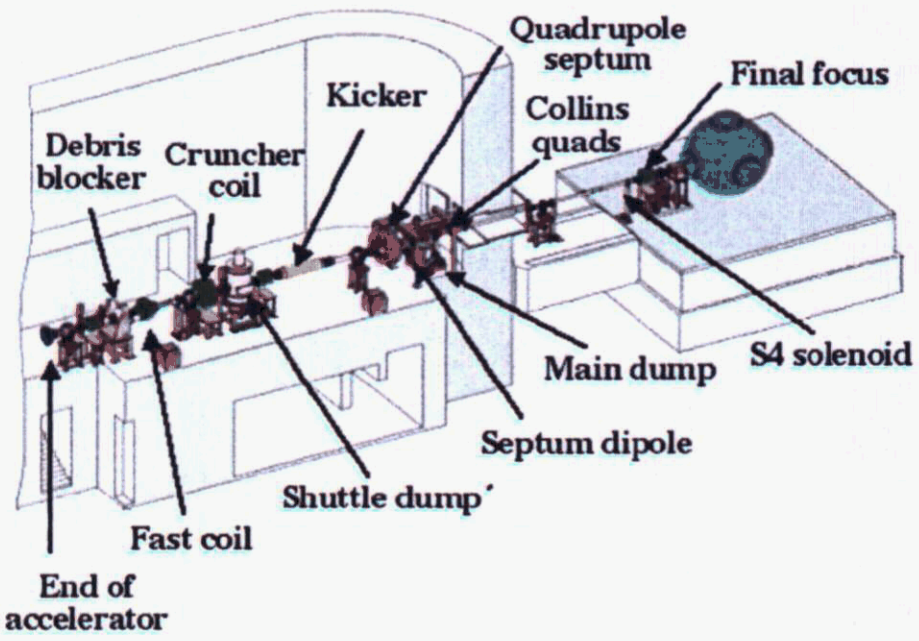

Figure 1: DARHT-II Downstream System

3 INSTABILITIES

The transport system is designed to minimize the transverse resistive wall instability and the ion-hose instability. Both of these mechanisms could potentially threaten the quality of the long pulse, high current beam in those long drift sections (~ 12 m) upstream of the quadrupole septum.

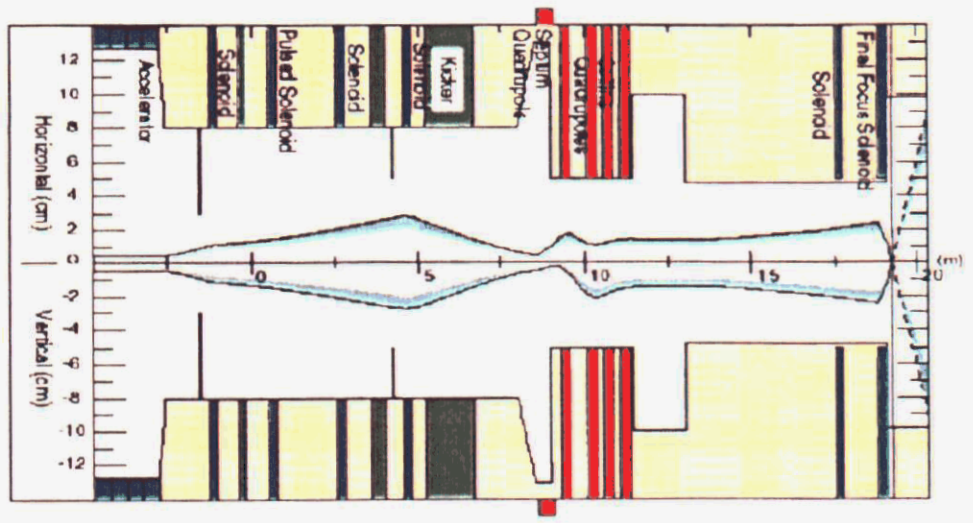

Figure 2: Beam envelope in the DARHT-II transport line from the accelerator exit to the target

The equation of motion for beam displacement $\xi(z, \tau)$ due to transverse resistive wall instability in a drift space is given as

$$\frac{\partial^2 \xi}{\partial z^2} = \frac{2}{\gamma\beta I_o} \frac{c}{\pi b^3 \sqrt{\sigma}} \int_0^{\tau} \frac{I(\tau)\xi(z,\tau')}{\sqrt{\tau - \tau'}} d\tau' \qquad (1)$$

Solving Eq. (1) yields

$$\xi(z,\tau) = \xi_o \sum_{m=0}^{\infty} \frac{\left(\alpha z \tau^{1/4}\right)^{2m}}{(2m)!\,\Gamma(1+m/2)} \qquad (2)$$

with

$$\alpha^2 \equiv \frac{2I}{\gamma\beta I_o} \frac{c}{b^3 \sqrt{\pi\sigma}} \quad , \qquad (3)$$

where I and I_o is the beam current and Alfven current, respectively, b is the wall radius, σ is the conductivity of the wall material, and c is the light speed. To minimize the transverse resistive wall instability in the mainly drift space upstream of the quadrupole septum, all transport components have large apertures, and most (70%) are made out of aluminum. The estimated amplification of the instability at the end of the 2 μs in this region is about 2 as shown in Fig. 3a. The materials for the components in the short pulse region (~ 10 m) are 90% aluminum. The instability in this region is caused by long-range residual wakefields. Since the time-averaged current over 2 μs is low, the instability growth is insignificant after the quadrupole septum (Fig. 3b). The four peaks shown in Fig. 3b are the real beam displacement during the beam pulses, and the gentle curve connecting the peaks indicates the growth due to the residual wakefields.

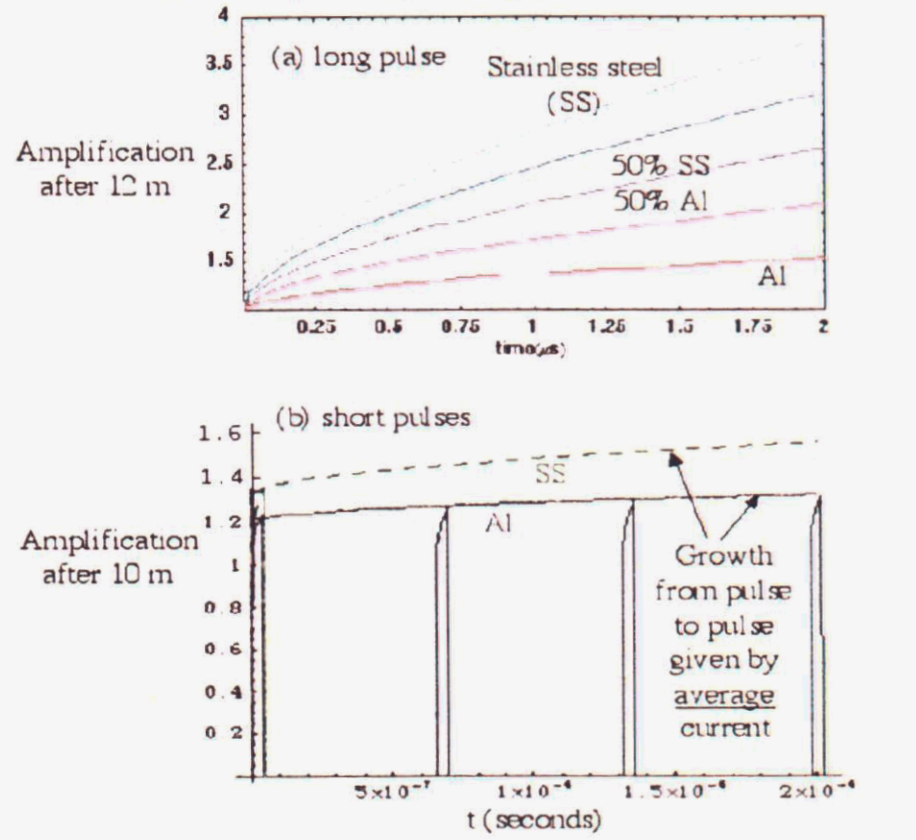

Figure 3: Amplifications of an initial beam offset caused by the transverse resistive wall instability for (a) the 2-μs beam transporting from the accelerator exit to the quadrupole septum and (b) the 4 short pulses travelling from the septum exit to the x-ray converter.

Since the DARHT-II accelerator will deliver a beam with a long beam head, the downstream transport line is designed to have a large beam acceptance. The beam head loss upstream of the kicker and beam loss at the septum during the kicker switching will deposit charge on the wall with the charge density on the order of nC/cm^2 and μC/cm^2 [6], respectively. These losses may lead to beam stimulated desorption. To minimize the focusing effects due to beam-induced ionization of the background gas, the average vacuum in the system is less than 10^{-7} torr. Reference [7] indicates that beam envelope variation has detuning effects on the ion hose instability in a continuously focusing system since the ion channel's oscillation frequency is determined by the beam's space charge forces which vary with the beam envelope size. We performed the analysis similar to that in Ref. [7] for a beam traveling in a drift space with a preformed ion channel, which has a Lorentzian ion frequency spread δ, by describing the envelope with a function $a[1+\mu\sin(\pi z/L)]$. The number of e-folding growth for a tickler excitation at the end of 12-m drift, varying with the envelope variation is shown in Fig. 4. Note that the DARHT-II long pulse beam's μ value (Fig. 2) is 5, which is greater than the maximum μ value, 2, shown in Fig. 4. The ion-hose instability is not a threat in the downstream system.

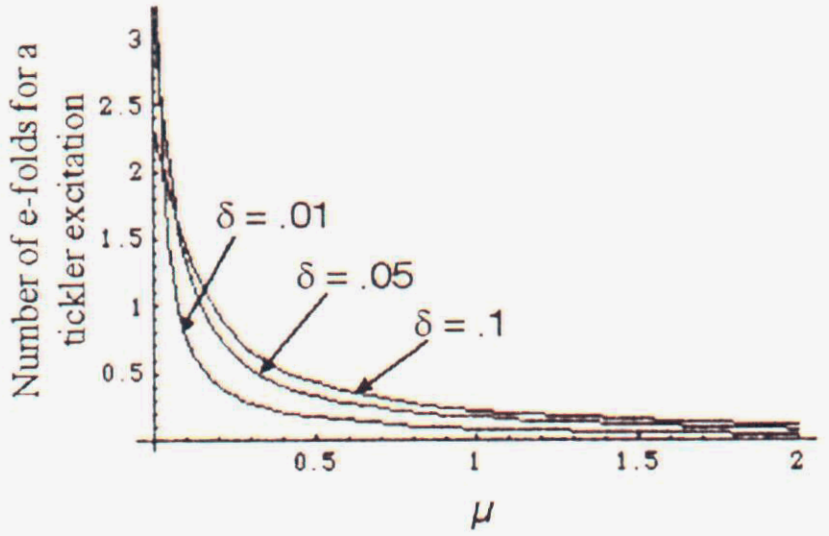

Figure 4: The number of e-folding growth for a tickler excitation of the ion-hose instability varies with the envelope variation parameter μ and the fractional ion frequency spread δ.

4 KICKER SWITCHING AND SPOT SIZE DILUTION

The DARHT-II kicker uses a modulated, solid-state high voltage pulser, which has multi-pulse burst capability

with very fast rise and fall times and pulse width agility [8]. The DARHT-II kicker ensemble has been tested successfully on the ETA-II accelerator at LLNL (Fig. 5). Both the kicked ETA-II beam [9] and the simulated, kicked DARHT-II beam [6] exiting the kicker ensemble, i.e., downstream of the Collins quadrupoles (Fig. 1), have a few nanoseconds of rise and fall. The kicker pulser's amplitude modulation and its control system can provide precision beam manipulation, such as compensating for transverse beam motion at the kicker input as well as the dynamic response and beam-induced steering effects associated with the kicker structure during the flattop portion of the kicker pulse for high current electron beams [9]. However, the transverse beam motion during the kicker pulser switching will not be compensated. The beam motion during the kicker switching is not an issue for a long pulse since its time integrated spot size on the target will be mainly determined by the beam in its flattop instead of by the beam in its head and tail. However, as demonstrated on the ETA-II (Fig. 6), kicker switching can potentially lead to dilution of the time integrated spot size for a short pulse. Without carefully tuning those quadrupoles downstream of the septum to minimize beam motion and displacement, every beam slice needs to be focused to a spot smaller than its nominal size in order to meet the radiography resolution requirements. A tighter beam will put DARHT-II's multi-pulse target's confinement at risk. Furthermore, a diluted time integrated spot is typically highly elliptical [6], which makes radiography analysis difficult. Fortunately, the spot size dilution can be eliminated with proper tuning of the Collins quadrupoles. The data for kicked beams in Fig. 6 were taken when 20-ns kicker pulses were applied to the center of the 40-ns ETA-II beam. Without an optimized tune, the time integrated beam over 100 ns shows the beam being kicked away from and back to its original spot. With an optimized tune to minimize the beam motion during the switching, there was little net beam motion over the entire beam even though the kicker pulser was on.

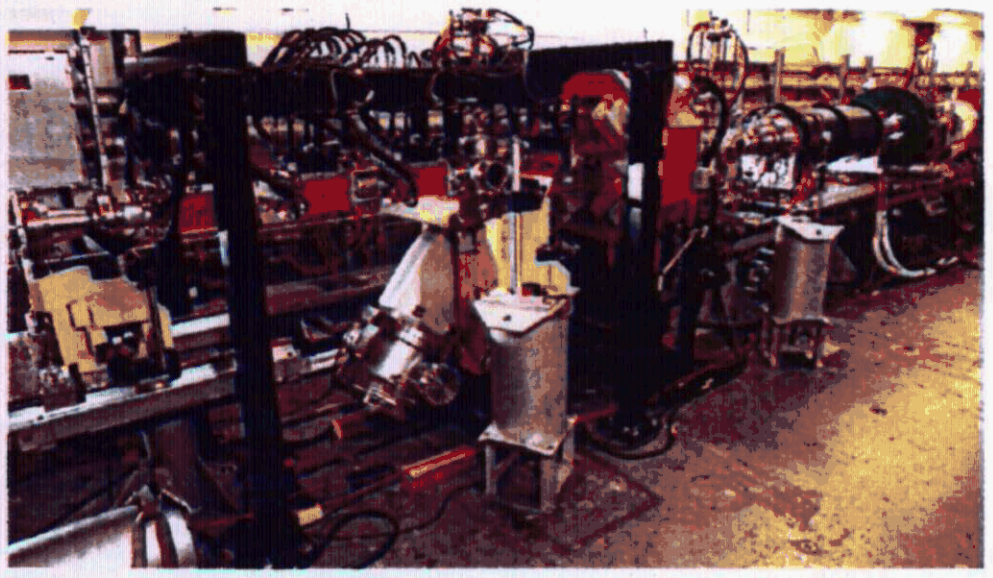

Figure 5: The DARHT-II kicker system being tested on the ETA-II accelerator.

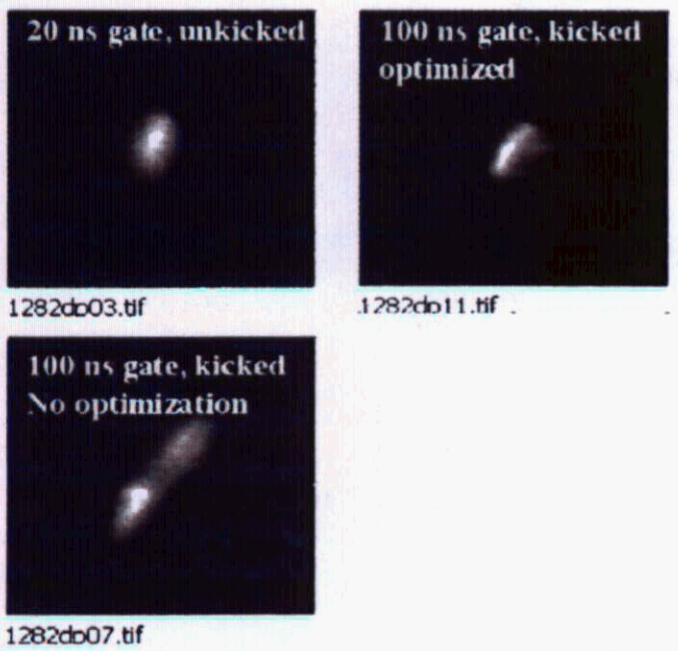

Figure 6: The time integrated ETA-II beam spots without the kicker pulser, and during the entire kicker switching with and without implementing the tuning optimization scheme.

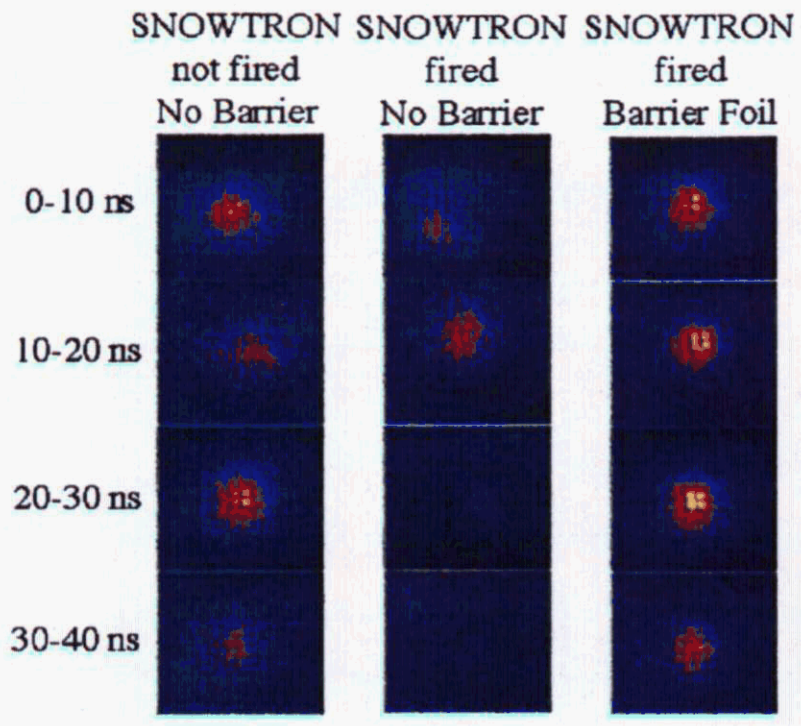

Figure 7: The x-ray spot sizes on the ETA-II/ SNOWTRON double-pulse foil-barrier experiment.

5 SPOT SIZE PRESERVATION

The strong electric field of the high current and high intensity electron beam may pull ions upstream from the desorbed gas at the target surface or from a pre-existing target plasma plume created by preceding pulses. The time varying focusing effects of those backstreaming ions can disrupt the beam spot size on the target. Hughes had suggested first to use a foil as a barrier to confine backstreaming ions within a short distance to minimize their focusing effects [11]. Mitigation of backstreaming ion effects with a foil-barrier was demonstrated on the ETA-II/SNOWTRON double pulses facility, which has been used to conduct target experiments for validation of the DARHT-II multi-pulse target concept [12]. To simulate the DARHT-II beam-target interactions, target plasma will be created first by striking the 1MeV, 2 kA Snowtron beam on one side of a target. The better characterized, 6 MeV, 2 kA ETA-II beam enters from the other side to probe the target. Without a pre-existing plasma created by the SNOWTRON beam, the spot disruption on the ETA-II beam due to the backstreaming ions was weak as shown in the left column in Fig. 7.

With the pre-existing plasma created by the SNOWTRON beam 600 ns earlier, the focus of the ETA-II beam was destroyed within 20 ns if a foil-barrier was not used as shown in the center column. However, if a foil was placed 1 cm in front of ETA-II sides target surface, the spot size was preserved through the entire ETA-II flattop as shown in the right column.

The DARHT-II target assembly consists of a distributed converter target and a foil barrier. The foil material and the beam spot size on the foil has to ensure survivability of the foil while it is being struck by four high current pulses over 2 μs. We have chosen graphite for the DARHT-II foil-barrier material. Figure 8 shows that the temperature of a 10-mil graphite will remain below its vaporization temperature at the end of 2 μs after the impact of all four DARHT-II pulses for a wide range of beam spot sizes on the foil. However, the foil temperature will be well above the threshold temperature (~ 400°C) for gas desorption. Therefore, the graphite foil's upstream surface can potentially become a backstreaming ion source if the graphite foil were not pre-cleaned before arrival of the beam pulses.

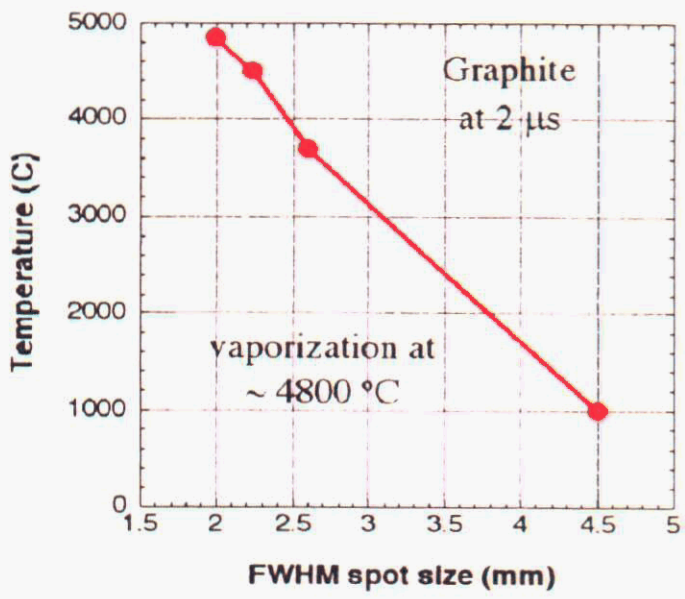

Figure 8: Temperature of the graphite foil after the impact of four DARHT-II pulses varying as the beam spot size on the foil.

We have investigated methods to pre-clean the graphite foil. A 6-mil graphite foil, which was backed with a 10-mil quartz foil, serving as an OTR witness foil, was used in the ETA-II laser cleaning experiment. A 60-mJ Nd:YAD laser at 1.06 μm was used to pre-clean the graphite. Since the backstreaming ions' spot size disruption effects on the ETA-II beam is weak without a pre-existing plasma (Fig. 7 and Fig. 9d). The laser was also used to create plasma on the graphite foil surface at 2 μs before the ETA-II beam was fired. The laser spot used for pre-cleaning was typically enlarged to about 5 mm in diameter. We found that the ETA-II spot was preserved if the separation between the last laser cleaning pulse and the ETA-II beam is around 1 second. Figure 9 shows that firing 9 or more laser pulses with large spots on the foil can effectively preserve the beam spot size through the entire beam flattop. Presumably those laser pulses have cleaned the graphite surface. The DARHT-II downstream system can accommodate laser cleaning for the foil-barrier.

Performance of the foil-barrier scheme for spot size preservation requires minimizing the backstreaming ions' focusing effects to a tolerable level. Since the ions' focusing forces are highly sensitive to the electron beam's envelope size, the beam spot size after a beam traveling through the ion channel in the foil-barrier is also sensitive to the beam envelope parameters. To reduce the spot size sensitivity, it is desirable to place the graphite foil as close to the target front surface as possible if the foil survivability were not a concern. The foil-barrier's performance can also be improved without sacrificing the final spot size and the x-ray dose by using a different focusing scheme to obtain a larger beam envelope in the ion trap region, which leads to weaker ion focusing forces and a larger beam spot on the foil [13]. A larger beam spot on the foil allows us to reduce the foil-target separation further, and hence, the beam's final spot size is further stabilized also.

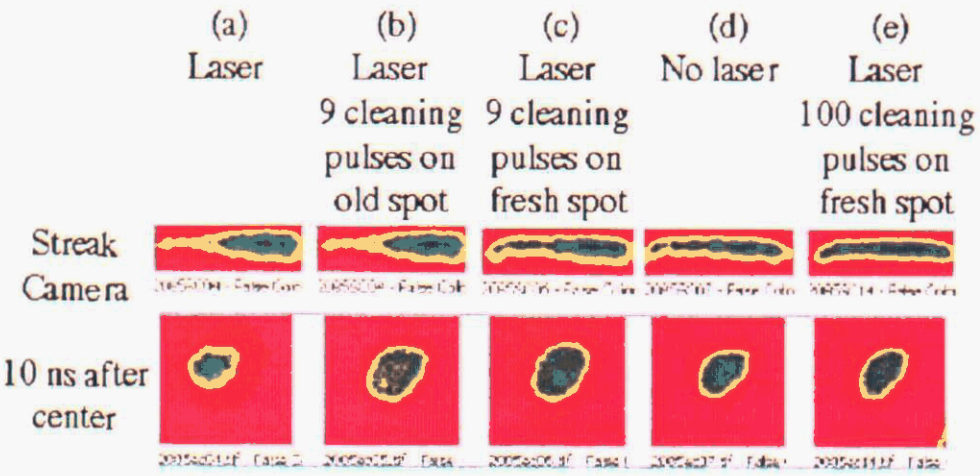

Figure 9: The ETA-II beam spot sizes corresponding to the number of pre-cleaning laser pulses.

6 X-RAY CONVERTER TARGET

Instead of using a conventional, solid Ta foil for the target, DARHT-II uses a distributed target [3], [4], [10], which distributes Ta over a distance. Scattering in the target and long separation between the target material lead to a large beam envelope inside the target. Hence, the deposited energy density is smaller inside a distributed target, which provides a reduced hydrodynamic expansion of the converter material so that there is enough material to generate four X-ray pulses with the required doses. By using the radiation hydrodynamics code, LASNEX, our modelling results of the DARHT-II target plasma hydro-expansion are shown in Fig. 10. The mass density at 0 μs is 3.95 g/c.c., and the lowest density contour value plotted is 10^{-10} g/c.c.. All beam pulses' spot sizes on the front target surface are 1.08 mm FWHM (Gaussian). Since the longest plasma channel, occurring at the onset of the 4th pulse, is only about 8 mm, the impact of the beam-plasma interactions on the x-ray spot size and dose is small. The simulated x-ray spot sizes and doses by using the Monte Carlo radiation transport code MCNP, shown

in Fig. 11, indicate that the target can meet its requirements.

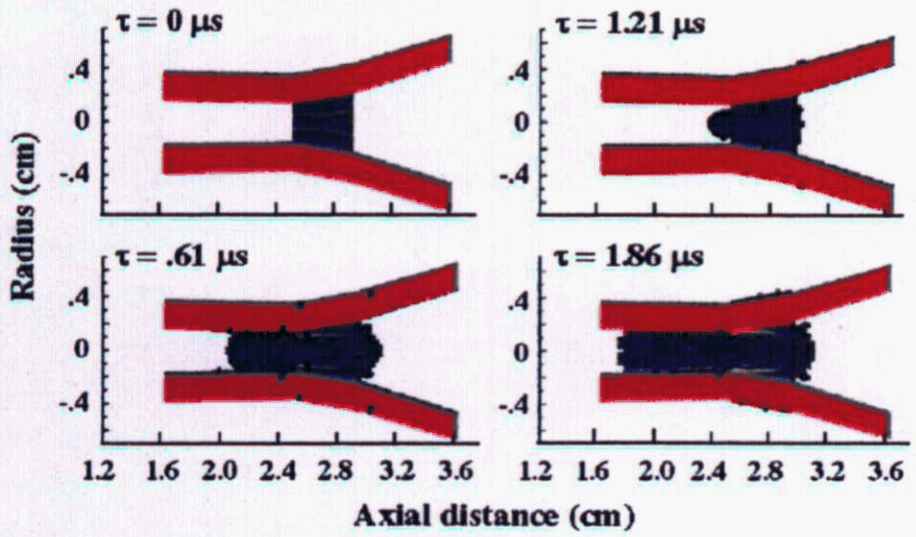

Figure 10: The DARHT-II target at the beginning of each pulse.

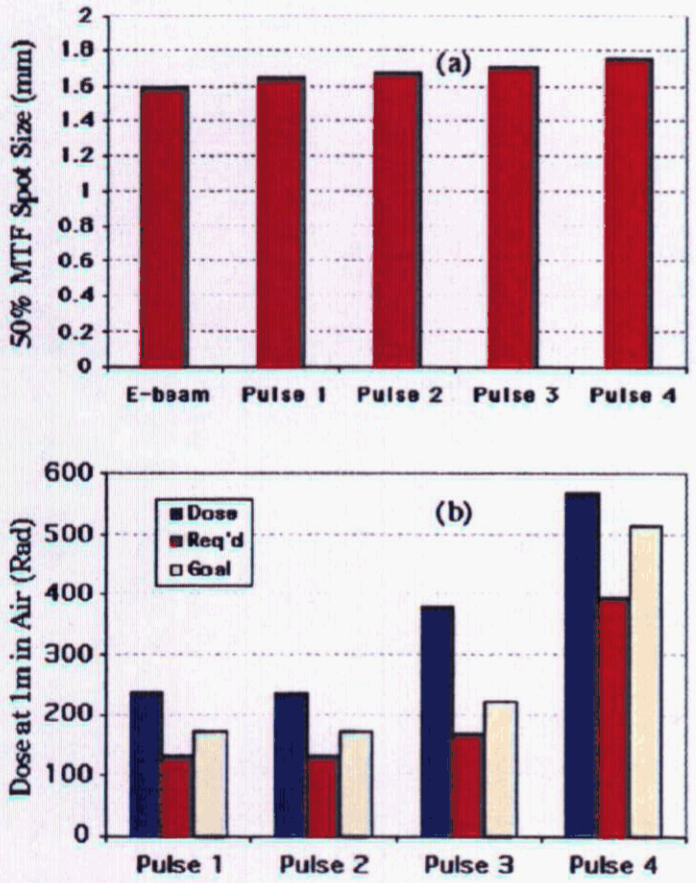

Figure 11: The DARHT-II x-ray (a) spot sizes and (b) forward doses.

7 SUMMARY

The DARHT-II downstream system will be the first system to transport a long pulse, high energy and high current electron beam, and the first system to deliver four selected 10-100 ns beam pulses to a novel, static x-ray converter target to produce high quality x-ray pulses for flash radiography. Preserving the beam quality in the entire system is essential for the radiography performance. We have shown that the transverse resistive wall instability and the ion hose instability will not threaten the quality of the DARHT-II beam. Furthermore, the DARHT-II transport system is equipped with many beam position monitors and steering dipole magnets for the beam centroid alignment. We have shown that the concern of spot size dilution due to kicker switching can be addressed with an optimizing magnetic tune, which minimizes the beam motion in the entire kicked beam pulse. We will use a foil-barrier to minimize spot size disruption caused by beam-target interactions. Based on our modelling, there are sufficient margins in the DARHT-II baseline target design to meet the performance needs. Therefore, any small dose reduction resulted from beam-target interactions, emittance growth or beam envelope divergence could potentially be compensated with a longer beam pulse length.

8 REFERENCES

[1] M. J. Burns, et. al., "Status of the Dual Axis Radiographic Hydrodynamics Test (DARHT) Facility", *Proc. of BEAMS 2002,* Albuquerque, NM, June 24-28, 2002.

[2] G. A. Westenskow, et. al., "The DARHT-II Downstream Transport Beamline", *Proc. of the 2001 IEEE PAC*, Chicago. IL, June 18-22, 2001, p.3487.

[3] Y.-J. Chen, et. al., "Downstream Transport System for the Second Axis of the Dual-Axis Radiographic Hydrodynamic Test Facility", *Proc. of the 14th High-Power Particle Beams,* Albuquerque, NM, June 24-28, 2002.

[4] Y. J. Chen, et. al., " Precision Fast Kickers for Kiloampere Electron Beams", *Proc. Of the 1999 IEEE PAC*, New York, NY, March 27 – April 2, 2002, p. 627.

[5] D. D.-M. Ho, Et. al., "Hydrodynamic Modelling of a Multi-Pulse X-Ray Converter Target for DARHT-II", LLNL Report. UCRL-JC-1442, July 26, 2001.

[6] B. R. Poole and Y.-J. Chen, "Particle Simulations of DARHT-II Transport System", *Proc. of the 2001 IEEE PAC*, Chicago. IL, June 18-22, 2001, p. 3299.

[7] G. J. Caporaso and J. F. McCarrick, "Ion Hose Instability in Long Pulse Induction Accelerator", *Proc. of the XX International LINAC Conference*, Monterey, CA, Aug. 21-25, 2000, p. 500.

[8] B. S. Lee, et. al., "Solid-State Modulated Kicker Pulser", *Proc. of the 2002 IEEE Power Modulator Conference*, Hollywood, CA July 1-3, 2002.

[9] J. A. Watson, et. al., "Control System for the LLNL Kicker Pulse Generator", *Proc. of the 2002 IEEE Power Modulator Conference*, Hollywood, CA July 1-3, 2002.

[10] P. A. Pincosy, et. Al., "Multiple pulse electron beam converter design for high power radiography", *Review of Scientific Instruments*, **72,** 2599-2604 (2001).

[11] T. P. Hughes, "Target Calculations for ITS Short-Focus Experiment", MRC/ABQ-N-589, September 1997.

[12] Y.-J. Chen, et. al., "Physics Design of the ETA-II/Snowtron Double Pulse Target Experiment", *XX International LINAC Conference*, Monterey, CA, Aug. 21-25, 2000, p. 482.

[13] Y.-J. Chen, et. al., "Final Focusing System for the Second Axis of the Dual-Axis Radiographic Hydrodynamic Test Facility", *Proc. of the 14th High-Power Particle Beams,* Albuquerque, NM, June 24-28, 2002.